Indian Journal of Radio & Space Physics
Vol. 23, June 1994, pp. 175-188

175-188

541.18

Effect of atmospheric relative humidity on aerosol size distribution

K Parameswaran & G Vijayakumar
Space Physics Laboratory, Vikram Sarabhai Space Centre, Thiruvananthapuram 695 022

Received 14 June 1993; revised received 10 November 1993

A method of accounting for the effect of variation in relative humidity on aerosol size distribution obtained from a low-pressure impactor (LPI) experiment is proposed. The size distribution of atmospheric aerosols under the prevailing relative humidities estimated by this method is compared with that obtained using a bistatic CW lidar. These results are used to study the effect of relative humidity on aerosol size distributions. At higher altitudes in the mixing region, increase in relative humidity causes a decrease in aerosol size index. The seasonal variation of aerosol number density near the surface is found to agree fairly well with the seasonal variation of the mixing region aerosol optical depth.

32-Ref

1 Introduction

Atmospheric aerosols, produced as a result of various natural and anthropogenic processes on the earth's surface, are essentially polydisperse having sizes ranging from one thousandth of a micrometre to a few tens of micrometres. Within this size range, the number of particles having a particular size varies with the particle size. Depending on the nature of this variation, different analytical functions are used to represent the aerosol size distributions[1-3]. A clear knowledge of the nature of this size distribution at any location is very important not only to characterize the atmospheric aerosol system over that location, but also to study the radiative properties[4] of the atomspheric region in which these aerosols are distributed. In addition, the chemical composition and size distribution of aerosols in the biosphere significantly influence the life on this planet. While soot, sulphureous and nitrogenous compounds, etc. are the important constituents of anthropogenic aerosols, the natural aerosols are constituted by wind blown dust (silica), sea-spray (sea-salt), and vegetative-originated pollens, seeds, etc. Even though the aerosols thus generated by different mechanisms get mixed and transported from place to place by the winds, their properties at a particular location primarily depend upon the relative strengths of these mechanisms. For example, while a coastal location like Thiruvananthapuram is manily dominated by sea-spray particles, an urban location will be dominated by anthropogenic particles. While aerosols of continental origin (silica and vegetative) are seen over the deep inland, arid regions are dominated by desert aerosols. Based on this the aerosols in the biosphere can be broadly classified as[3] urban, rural, maritime, oceanic, continental, etc.

Even though atmospheric aerosols are generally hygroscopic, the soot contained in the anthropogenic aerosols has very little affinity for water. The water affinity of aerosols vary with the aerosol type (or composition). When relative humidity (RH) increases, depending on the water affinity more atmospheric water vapour condenses on the particles. This process not only makes the particles to grow in size but also changes their composition and effective refractive index. Thus, changes in the atmospheric humidity can significantly alter the radiative characteristics of these aerosols.

There have been a number of studies on the changes in aerosol properties as a function of relative humidity[5-10], of which the most comprehensive one is the work of Hanel[10] who established an empirical relationship for the growth of aerosol particle as a function of relative humidity. The amount of this growth for a given humidity change depends on the water activity of the aerosol type.

2 Relevance of the present study

Study of the size distribution of atmospheric aerosols includes a variety of techniques involving both direct sampling[11-13] as well as remote sensing[14,15] methods. At the coastal station Thiruvananthapuram (8.55°N, 77°E), we have carried out investigations on aerosol size distributions employ-

ing both these techniques; the preliminary results of our investigations were presented in an earlier communication[16]. In obtaining the size distribution from direct particle sampler, it is usually assumed that the aerosols are homogeneous in density throughout the size range of interest. A prior knowledge of this density is required for the estimation of the Stokes diameter. This is taken as 2.5 g cm^{-3}, which is generally true for dry maritime and continental aerosols[17,18]. As atmospheric relative humidity increases, more and more water vapour condenses on aerosol particles, resulting in a decrease of the effective particle density. This decrease of particle density with increase in RH should be accounted appropriately in obtaining the aerosol size distribution from the low-pressure impactor (LPI) experiment. In addition, the collection substrates are desiccated before weighing to eliminate the effect of direct condensation of atmospheric water vapour on these substrates. In this process the particles collected on these substrates also will lose some of their water content. Thus, even though the particles are collected according to their sizes prevailing in the atmosphere, on desiccation they change their size and composition according to the relative humidity condition prevailing inside the desiccator. These effects are also to be accounted in obtaining the size distribution of aerosols. In this communication we report the results of these studies along with the effect of atmospheric relative humidity on the observed size distribution obtained using the LPI and bistatic CW lidar experiments.

3 Experimental set up and method of obtaining aerosol size distributions

Two experiments, viz. a bistatic CW lidar (CWL) and a low-pressure impactor are used to study the size distribution of atmospheric aerosols. The CWL system consists of a laser transmitter (wavelength, 514.5 nm) and a transmission-type receiving telescope separated by a fixed distance of 380 m in the same horizontal plane. The laser beam is transmitted along a slant path and the angularly scattered intensity from a fixed altitude (~ 190 m) is measured for different scattering angles by suitably orienting the transmitter and receiver beam directions. From this measurement of the angular distribution of scattered intensity, the size index of aerosol distribution (assuming the basic form to be of modified power law[19] type) is obtained[20]. As this experiment is essentially a remote sensing type, the sensed particles do not lose their identity. The basic form of the size distribution is assumed which is to be ascertained by a complimentary supporting experiment.

The LPI (Andersen LPI model 20-900) is used as the complimentary experiment (of CWL) for studying the mixing region aerosol size distribution. It consists of 14 collection stages with 6 size ranges below 1.0 μm. Each stage of the LPI has a number of small perforations (nozzles) below which the collection substrate is suitably arranged. Air containing aerosols are forced through these nozzles and allowed to impinge on this substrate, where particles above a certain size (determined by the cut-point of that stage) will be collected with 50% efficiency and all sizes below this size will be passed without collection. The size of these nozzles (jets) determining the speed of the air for a constant suction rate decreases in subsequent stages from dimensions of several millimetres at the initial stages to tenths of millimetres at the final stage. When a number of such stages are properly cascaded, each stage collects particles having sizes ranging between its cut-point and that of its previous stage. The jet diameter (D_j) and jet velocity (V_j) for the recommended operating condition of the LPI (critical orifice pressure of 114 torr) as provided by the manufacturer for each of the impactor stages are presented in Table 1 along with the respective Stokes numbers (S_j). The mass of particles collected in each size range is obtained by subtracting the tare mass of each substrate from its final mass. This is used for estimating the mass distribution of the sampled aerosol particles.

Table 1—Values of the jet diameter (D_j), jet velocity (V_j), Stokes parameter (S_j) and the aerodynamic cut-points of different LPI stages

LPI stage	D_j cm	V_j cm/s	S_j	Aerodynamic cut-point μm
0	0.2550	10.2	0.297	>35
1	0.1887	18.6	0.283	21.7
2	0.0914	19.1	0.315	15.7
3	0.0711	31.5	0.303	10.5
4	0.0533	56.1	0.289	6.6
5	0.0343	135.1	0.275	3.3
6	0.0254	246.3	0.265	2.0
7	0.0254	485.4	0.252	1.4
L1	0.0914	1949	0.250	0.90
L2	0.0533	2415	0.250	0.52
L3	0.0533	5747	0.245	0.23
L4	0.0343	8546	0.245	0.11
L5	0.0254	9009	0.247	0.08
LF	—	—	—	<0.08

4 Estimation of the LPI cut-points

The cut-points of different impactor stages are estimated from the respective values of D_j, V_j and S_j using the relation[21]

$$D_p = \left(\frac{9\mu S_j D_j}{\rho C V_j}\right)^{1/2} \quad \ldots (1)$$

where

$$\mu = (63 + 0.40\,T) \times 10^{-6} \quad \ldots (2)$$

is the viscosity of air (P) at the atmospheric temperature T (K), ρ the particle density (g cm^{-3}), and C the Cunningham slip correction factor for a particle having diameter D_p and is given by

$$C = 1 + 1.257\left(\frac{2L}{D_p}\right) \quad \ldots (3)$$

where

$$L = \frac{82.057\,\mu T}{0.499\,PM\sqrt{\frac{8R_g T}{\pi M}}}, \quad \ldots (4)$$

is the mean free path, P the atmospheric pressure (atm), M the mean molecular weight of air (28.9), and R_g the gas constant (8.31×10^7).

In Eq. (1), D_p represents the aerodynamic cut-point (particle diameter) D_a of each stage if the particle density ρ is assumed to be 1.0 g cm^{-3}. The aerodynamic diameter is defined as the diameter of a unit density sphere with the same terminal settling velocity as the particle. If the actual particle density is used for ρ in Eq. (1), the resultant D_p is referred to as the Stokes cut-point (D_s), defined as the diameter of the sphere with same density as the particle which would behave in the impactor in the same way as the particle (i.e. the diameter of a sphere of the same density as the particle with the same terminal settling velocity) of that stage. Thus the Stokes diameter, which is closer to the physical diameter (assuming spherical), can be calculated if the actual density of the aerosol particle is known.

In Eq. (1) for calculation of D_p, the slip correction factor, C, appearing in the denominator is also a function of D_p as given by Eq. (3). Then Eqs (1) and (3) are to be solved through iteration. To start with, C is taken as unity and D_p is estimated using Eq. (1). This is used to estimate the actual value of C using Eq. (3) which again is substituted back in Eq. (1) to re-estimate D_p. This iteration process of estimating D_p, by repeatedly correcting the value of C, is continued till the values of D_p obtained at the end of two successive iteration, converge within 0.001%. As the first eight stages (0 to 7) of the LPI are operated at the atmospheric pressure itself, the value P in Eq. (4) for these stages is 1 atm. For the remaining six-low pressure stages (L_1 to L_F) the value of P is 0.15 atm, which corresponds to the standard critical orifice pressure of 114 torr. The aerodynamic cut-points obtained using this procedure (Table 1) are in agreement with the values reported by the manufacturer[16].

The LPI collects particles from the atmosphere by continuous suction of ambient air. The system is operated during the daytime from 0900 to 1630 hrs IST for about 6 days to collect measurable aerosol samples. The atmospheric relative humidity generally remains steady during this period (within ±5%). But this will not be true from one sample to the other because of the seasonal variation in atmospheric relative humidity. During the monsoon months the atmospheric relative humidity will be (80-90%) higher than that during the winter (50-60%) months of December to February. The particles are graded and collected according to their sizes under prevailing relative humidities. After collection, the substrates are unloaded from the LPI and desiccated for ~24 h. The relative humidity inside the desiccator will be ~45% which is lower than the prevailing atmospheric value at any time. The weighing also is performed in a low relative humidity environment (which is almost the same as that in the desiccator environment). As the particle size decreases with decrease in relative humidity[10], the upper and lower size limits of the particles collected in each substrate will be less than that during the collection (determined by the impactor cut-points). Thus on desiccation the mean size as well as the size interval of particles in each collection substrate decreases from its actual value during the collection. In order to obtain the true size distribution, the desiccated particles should either be transferred to the actual atmospheric relative humidity condition before weighing, or the change in particle size and composition due to desiccation should be accounted appropriately.

5 Effect of relative humidity on aerosol size and density

As the relative humidity increases, aerosol particles grow in size due to condensation of water vapour from the atmosphere. This change in parti-

cle size with relative humidity can be estimated based on the semi-empirical models developed by Hanel[10] for different aerosol types. According to this model, the change in the particle size is related to the relative humidity through the relation

$$r_R = r_0 \left[1 + \rho_0 \frac{m(\mathrm{w})}{m_0} \right]^{1/3} \quad \ldots (5)$$

where r_0 is the dry particle radius, ρ_0 the particle (dry) density relative to water, m_0 the dry particle mass, $m(\mathrm{w})$ the mass of condensed water (on the aerosol particle) which is a function of the relative humidity R, and r_R the particle radius at the relative humidity R. The amount of condensed water $m(\mathrm{w})$ depends on the water activity (a_w) of the aerosol particle which is given by

$$a_w = R \exp \left[- \frac{2 \sigma V_w}{R_w T r_R} \right] \quad \ldots (6)$$

where σ is the surface tension on the wet particle surface, V_w the specific volume of water, and R_w the specific gas constant for water. The value of $2 \sigma V_w / (R_w T)$ at 300 K is ~0.00105 μm. Hanel[10] has tabulated $m(\mathrm{w})/m_0$ versus a_w for various types of natural aerosols. However, even with this data on the relative mass of condensed water for use in Eq. (5), it is not possible to combine Eqs (5) and (6) into an exact analytical expression giving aerosol radius, r, as an explicit function of relative humidity because r_R is also a function of a_w. To avoid limitation of approximation starting with $a_w = R$ on the right hand side of Eq. (5), Eqs (5) and (6) are used alternatively in an iterative manner until they converge. Starting with $r = r_0$ in Eq. (6) also leads to the same result. Thus using Eqs (5) and (6) the value of r_R for any relative humidity can be estimated for a given value of the particle size at a given relative humidity condition. Once the wet aerosol particle size is estimated from Eqs (5) and (6), the effective density ρ_R of the particle at a relative humidity R is simply the volume weighted average of the densities of dry aerosol (ρ_0) and water (ρ_w). This can be written as

$$\rho_R = \rho_w + (\rho_0 - \rho_w) \left(\frac{r_0}{r_R} \right)^3 \quad \ldots (7)$$

This can also be written in terms of the mass ratio of condensed water and dry particle mass as[10]

$$\rho_R = \rho_0 \left[\frac{1 + \dfrac{m(\mathrm{w})}{m_0}}{1 + \dfrac{m(\mathrm{w})}{m_0} \left(\dfrac{\rho_0}{\rho_w} \right)} \right] \quad \ldots (8)$$

in which $m(\mathrm{w})/m_0$ is a function of water activity a_w. The mass of aerosol particle at a relative humidity R, denoted by m_R, can be written as

$$m_R = m_0 + m(\mathrm{w})$$

or

$$m_R = m_0 \left(1 + \frac{m(\mathrm{w})}{m_0} \right) \quad \ldots (9)$$

Thus, knowing the water activity of the aerosol particles, the effective density and mass of the particle at any relative humidity can be estimated from its dry density and dry mass using Eqs (8) and (9). Conversely, the dry mass of the particle can be estimated from the humid mass m_R knowing a_w. Eq. (9) can also be written in terms of the particle radii and dry density as

$$m_R = m_0 \left[1 + \left(\frac{\rho_w}{\rho_0} \right) \left\{ \left(\frac{r_R}{r_0} \right)^3 - 1 \right\} \right] \quad \ldots (10)$$

The above relationship obtained for single aerosol particle is true for a group of n homogeneous particles having same mean radius and water activity.

6 Estimation of aerosol size distribution from LPI and correction for relative humidity

The method of collection of aerosol samples using the LPI is detailed in our earlier publication[16]. The LPI is operated during the daytime on 6-8 days in a month with rain free-fair weather conditions prevailing to collect measurable aerosol samples. In the monsoon season, the LPI is operated during the break-monsoon period. The mass of aerosol particles collected in each LPI stage ($\mathrm{d}m_s$) is obtained from the tare and final masses of the respective stage substrate, and corresponds to a relative humidity of 45% prevailed in the desiccator environment. The dry density of these particles is taken as 2.5 g cm^{-3} which is applicable for a marine station[18] like Thiruvananthapuram. The average relative humidity during the sampling is obtained from the hourly values of RH in that period.

Figure 1 shows a plot of the mass of aerosol particles collected ($\mathrm{d}m_s$) in different LPI stages (1 to L5) for each sampling cycle versus the mean

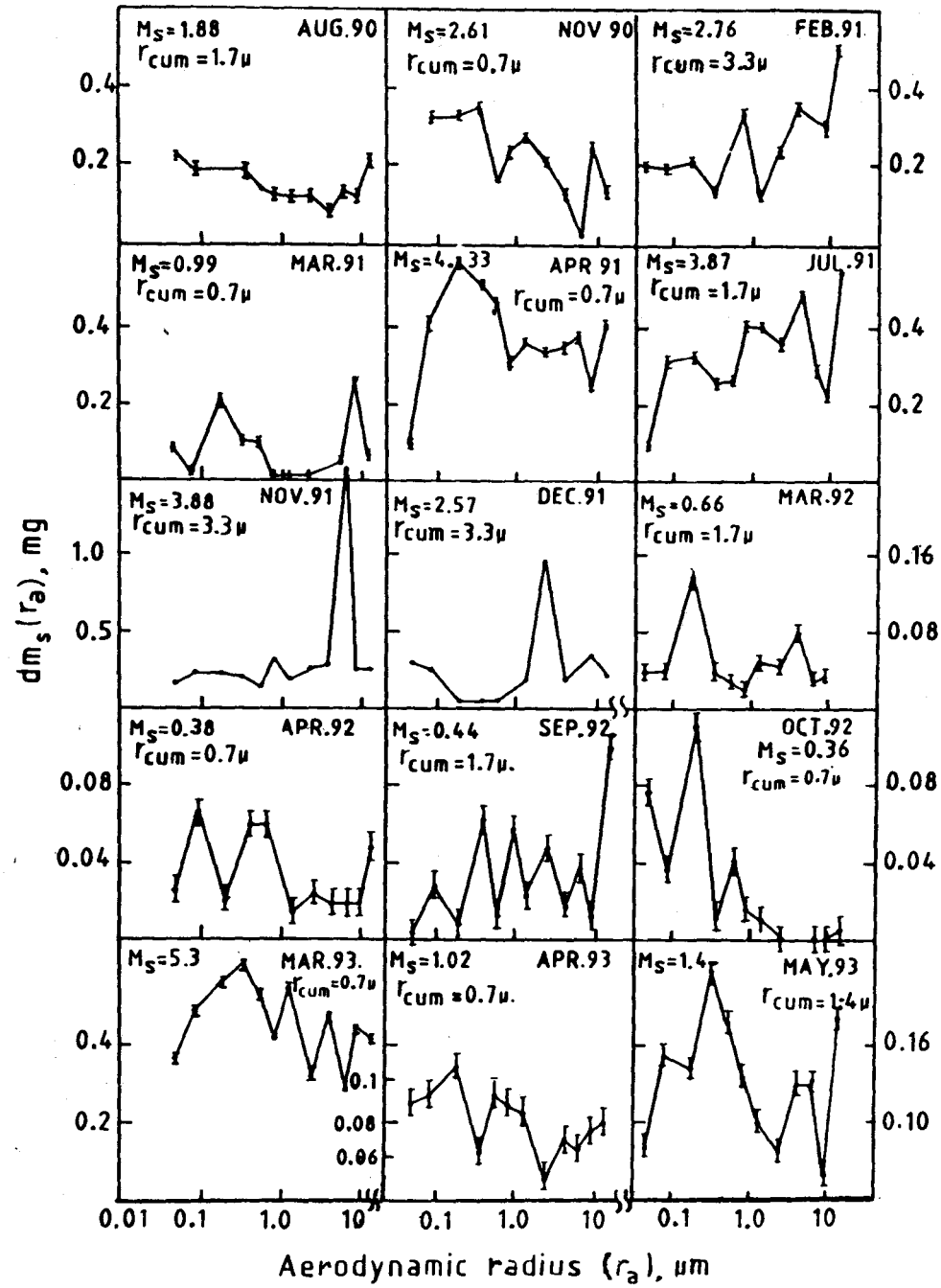

Fig. 1—Plots of the aerosol mass collected in different LPI stages versus the mean aerodynamic radius.

aerodynamic radius (r_a). As the '0' stage has no upper limit and the backup stage 'LF' has no lower limit, these stages are excluded from this plot as well as for further analyses (except for the cumulative percentages). Total mass of particles collected (M_s, in mg) in all these stages (aerosol mass loading) is shown in the respective frames of Fig. 1. Vertical lines in these figures show the error in dm_s due to the uncertainity (± 5 μg) in weighing the substrates. As the mass loading varies by an order of magnitude from sample to sample, expanded scales are used to represent dm_s for months in which the mass loading is small. Those months for which the mass loading is large and hence compressed scales are used, the error bars are too small to be displayed. Due to this reason error bars are not displayed for the curves corresponding to November 1991 and December 1991. Separate scales are used for the set of figures in each row (of Fig. 1) and the panels in the same

row for which there is a change in scale (of dm_s), are indicated by a break on the X-axis. The scale for r_a is logarithmic and is same for all the panels. The shape of the curve varies significantly from month to month. The mass loading is generally small during 1992 compared to the other three years. It is quite large in April 1991 and in March 1993. As will be seen later, increased mass loading in April 1991 is not due to an increase in aerosol number but owing to the low value of the prevailing relative humidity, the particles were more denser (compared to July 1991) in this month. But the increased mass loading in March 1993 is reflected in the aerosol number density also.

From the mass of aerosol particles collected in each stage, the cumulative percentage mass for aerosols more than a particular size is estimated[16]. The mass median aerodynamic radius (r_{cum}) for which the cumulative percentage is ~ 50% (including stages '0' and 'LF' is given in Fig. 1 along with the respective plot of dm_s. Larger values of r_{cum} indicate dominance of larger-size particles or decrease in small-size particles. The large r_{cum} values observed in the months of November and December 1991 are due to excessive mass-loading in the aerodynamic size range 5-7 μm during these months.

Figure 2 shows the mass median distribution obtained by dividing $dm_s(r_a)$ with the logarithm of the aerodynamic size range of the respective stage $[dm_s(r_a)/d\log r_a]$ versus the aerodynamic particle size (r_a). It should be noted from Table 1 that the value of $d\log r_a$ is not the same for all the LPI stages and decreases with decrease in r_a. The vertical lines showing the error bars due to the uncertainty in $dm_s(r_a)$ are more distinct when the Y-axis scale is large. These distributions generally show a maximum between 0.1 and 1 μm (not observed in November 1991) and a minimum around 2 μm. A secondary enhancement in $dm_s(r_a)/d\log r_a$ is observed for larger size particles around 10 μm.

Using the three available information on the characteristics of the aerosol particles, viz. the dry density, mass of aerosols in different size ranges (dm_s) and the aerodynamic cut-points of each stage, and the relative humidity dependence of various parameters given above, it is possible to obtain the size distribution of aerosols under the prevailing relative humidity R. This essentially involves an iterative procedure connecting the aerodynamic diameter, effective density, the Stokes diameter and mass of particles collected in each of the LPI stages (dm_s); the details of which are given below.

To start with, the aerodynamic cut-points of each LPI stage is estimated using the appropriate values of D_j, V_j and S_j (given in Table 1) employing Eq. (1) keeping $\rho = 1$ g cm^{-3}. The lower and upper aerodynamic size limits of particles collected on different substrates (at RH = R) are respectively the aerodynamic cut-points of the particular stage and that of its previous stage. From these the respective lower and upper size limits of the particles in each substrate at the dry condition (RH = 0) and at the desiccated condition (RH = 45) are estimated using Eqs (5) and (6). Hanel's tables[10] connecting $m(w)/m_0$ and a_w applicable for marine aerosols are used for this purpose. The mean diameters corresponding to the three relative humidities (0, 45 and R) are estimated by averaging the respective lower and upper size limits of each stage substrate. Half of these diameters give the corresponding radii. As a first approximation these aerodynamic radii are taken as the physical radii of particles at RH = 0, RH = 45 and RH = R (say r_0, r_s and r_R respectively) and using Eq (7) the effective particle densities are computed for RH = 45 and RH = R (say ρ_s and ρ_R respectively) with $\rho_0 = 2.5$ g cm^{-3}. The upper and lower Stokes radii limits and hence the mean Stokes radius (r_R) of each LPI stage is calculated by substituting $\rho = \rho_R$ in Eq. (1) for RH = R. This is used to re-estimate the mean radius of particles in this LPI stage for the dry condition (r_0) and desiccated condition (r_s) using Eqs (5) and (6). This is repeated for different LPI stages to give a set of second order values for r_0, r_s and r_R. These Stokes radii which are more closer to the physical radii of the particles in the respective stages are used to re-estimate the effective densities, ρ_s and ρ_R using Eq. (7). The resulting new values of ρ_s and ρ_R are again used to estimate a set of third order values of r_0, r_s and r_R. This process is continued until the corresponding values for ρ_s and ρ_R (and hence for r_s and r_R) on two successive iterations converge within 0.1%. Usually 5 to 6 iterations were found to be necessary to achieve the desired convergence.

The dry aerosol mass (dm_0) at RH = 0 and the humid aerosol mass (dm_R) corresponding to RH = R can be estimated from the measured mass (dm_s) using Eq. (9), knowing the water activity of the aerosol particles (a_w) corresponding to sizes r_s and r_R and Hanel's (ref. 10) tables connecting $m(w)/m_0$ with a_w. These quantities can also be

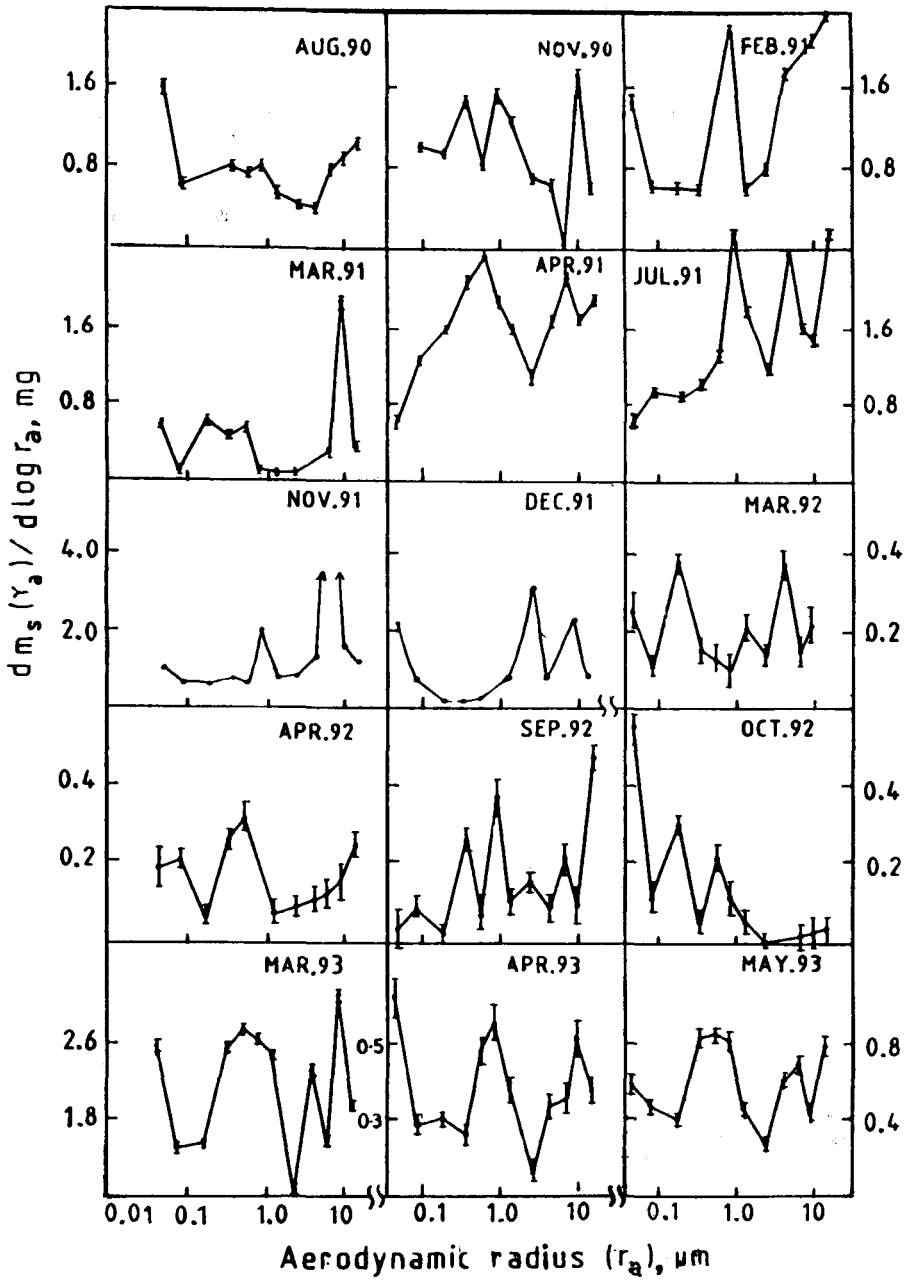

Fig. 2—Plots of mass median distribution (logarithmic) of aerosol samples versus the mean aerodynamic particle size.

estimated using Eq. (10) by substituting the known values of ρ_0, ρ_s, ρ_w, r_0, r_s and r_R. In our estimates, we have employed Eq. (10) for the computation of dm_0 and dm_s. The mass distribution of aerosols at the three relative humidities (RH = 0, RH = 45 and RH = R) are obtained by dividing the respective masses by the corresponding Stokes radii intervals (the difference between the upper and lower Stokes radii limits of particles in each LPI stage at the respective relative humidities obtained at the end of iteration process) denoted by dr_0, dr_s and dr_R respectively.

The number-size distribution of aerosols at the prevailing humidity (R) is thus obtained from dm_R as[16]

$$\frac{dn_R(r_R)}{dr_R} = \frac{3}{4\pi r_R^3 \rho_R} \frac{dm_R(r_R)}{dr_R} \quad \ldots (11)$$

where $dn_R(r_R)$ is the number of aerosol particles in the radius range r_R and $r_R + dr_R$ at the prevailing relative humidity R.

Similarly the number-size distribution corresponding to dry as well as desiccated conditions for these aerosols can also be obtained from the respective mass distributions. For dry condition

$$\frac{dn_0(r_0)}{dr_0} = \frac{3}{4\pi r_0^3 \rho_0} \frac{dm_0(r_0)}{dr_0} \quad \ldots (12)$$

and for desiccated condition

$$\frac{dn_s(r_s)}{dr_s} = \frac{3}{4\pi r_s^3 \rho_s} \frac{dm_s(r_s)}{dr_s} \quad \ldots (13)$$

In Eqs (12) and (13), $dn_0(r_0)$ represents the number of aerosol particles in the radius range r_0 and $r_0 + dr_0$ for the dry condition, which becomes $dn_s(r_s)$ in the radius range r_s and $r_s + dr_s$ for the desiccated condition.

To delineate the effect of relative humidity, the variation of the lower Stokes radius limit of particles collected at 95% relative humidity with decrease in RH is shown in Fig. 3(a) along with the corresponding variation in particle density (ρ_R) with RH [Fig. 3(b)] for a value of $\rho_0 = 2.5$ g cm^{-3} in the dry condition. In obtaining these radius limits for each RH in Fig. 3(a), the variation of particle density with RH represented by Fig. 3(b) is taken into account. The upper Stokes radius limit of any stage is the same as the lower Stokes radius limit of the previous stage. As the sampling is made at 95% relative humidity, the limiting radius corresponding to RH = 95% represents the respective Stokes cut-point of that stage estimated using Eq. (1) with the appropriate value of ρ (= 1.15 g cm^{-3}) at this relative humidity. The subsequent size limits represented by each curve for lower values of RH show the decrease in the size of these collected particles in a particular LPI stage with decrease in RH, obtained using the Hanel's relations, Eqs (5) and (6). Table 2 shows the typical values of the mean particle radii and radius intervals for stages 1 to L5 corresponding to the size limits shown in Fig. 3(a) for the two extreme cases of relative humidities RH = 0 and RH = 95%. As the variation of particle size with humidity is small for RH < 50% [seen from Fig. 3(a)], the values of these two parameters corresponding to RH = 45% will be close to (but slightly greater than) the corresponding values at RH = 0. The decrease in mean radius and radius interval with decrease in RH is evident from this table. Taking the mass of particles collected in each LPI stage at RH = 45% in a sampling process (on July 1991) as reference, its variation with RH estimated using the above relationships is presented in Fig. 4. The stage for which each curve corresponds is marked along the respective curve. The mass loadings in stages 7 and L1 were almost the same and hence in Fig. 4 curves corresponding to these two stages overlap. Figures 3 and 4 clearly depict the effect of desiccation on particle size and particle mass.

7 Discussion of the results

The above procedure was adopted to estimate the number-size distribution of aerosol samples collected in different months during the period 1990-93. A typical plot of the size distribution obtained for August 1990 is presented in Fig. 5 for

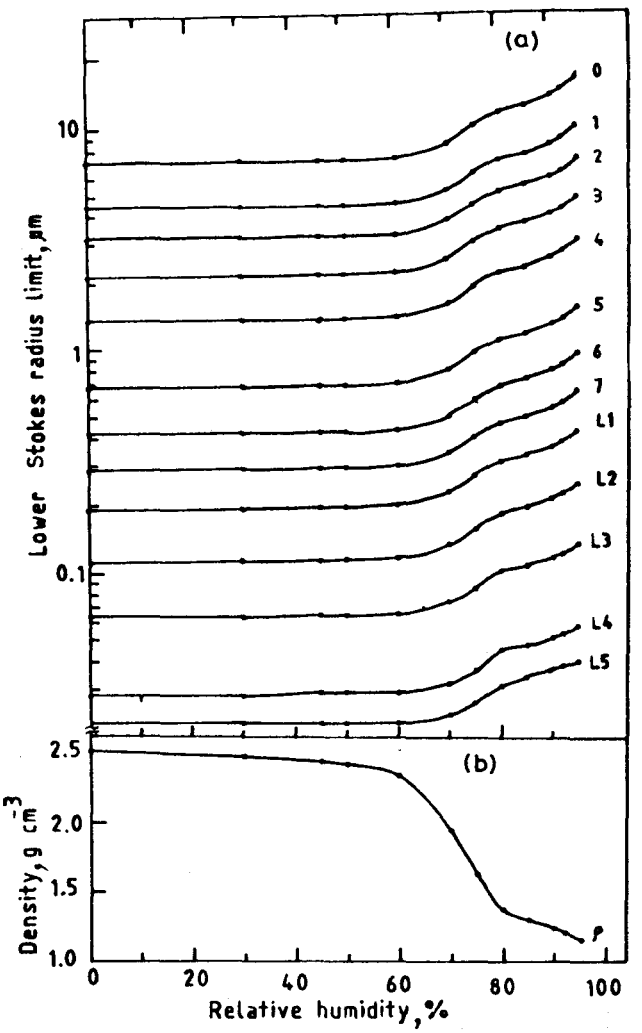

Fig. 3—(a) Variation of the LPI cut-points (lower Stokes radius limits) with relative humidity (RH); (b) variation of particle density (ρ) with relative humidity for a dry density of 2.5 g cm^{-3}.

dry, desiccated and ambient relative humidity conditions respectively. The prevailing mean atmospheric relative humidity during the sampling period was 89 ± 5%. The general form of curve is the same for the three RH conditions. The lower and upper size limits of the distribution increase with increase in RH. The values of size indices obtained for RH = 0, RH = 45 and RH = 89, considering the full size range in each case, are 4.04, 4.04, 4.0 respectively. There is a small decrease in the value of the size index (though not significant considering the error bars) at the actual atmospheric con-

Table 2—Mean Stokes radii and radius intervals for dry (RH = 0) and humid (RH = 95%) conditions corresponding to the size limits shown in Fig. 3(a)

LPI stage	RH = 0%		RH = 95%	
	Mean Stokes radius μm	Radius interval μm	Mean Stokes radius μm	Radius interval μm
1	5.75	2.69	13.35	6.25
2	3.8	1.22	8.82	2.82
3	2.67	1.05	6.18	2.43
4	1.75	0.78	4.05	1.83
5	1.02	0.684	2.35	1.58
6	0.55	0.257	1.25	0.60
7	0.35	0.133	0.81	0.306
L1	0.24	0.095	0.54	0.183
L2	0.15	0.080	0.34	0.128
L3	0.084	0.055	0.19	0.064
L4	0.042	0.028	0.089	0.017
L5	0.024	0.007	0.048	0.016

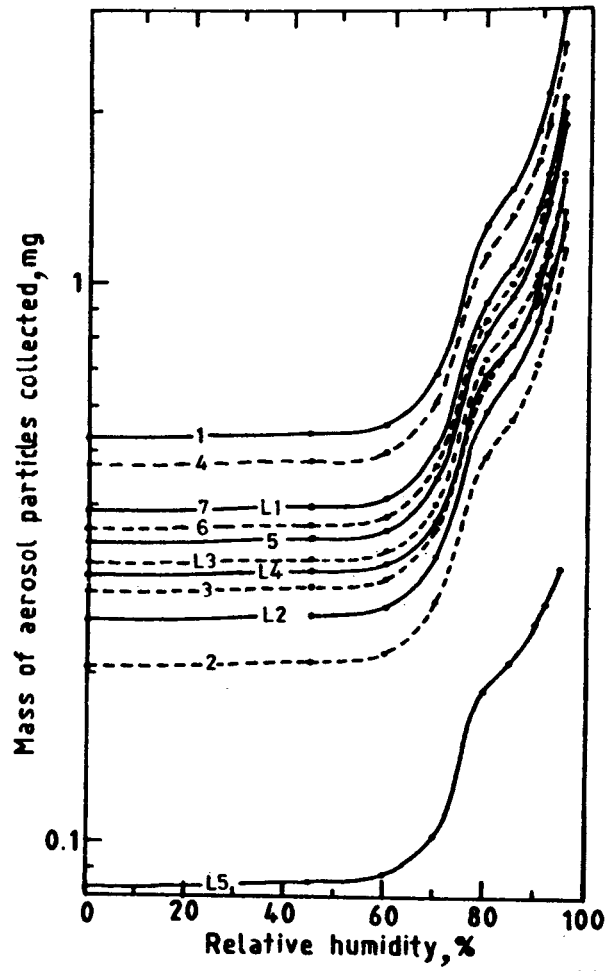

Fig. 4—Typical variation of the mass of particles collected in different LPI stages with relative humidity (RH) taking the mass of desiccated samples (at RH = 45%) collected on July 1991 as reference.

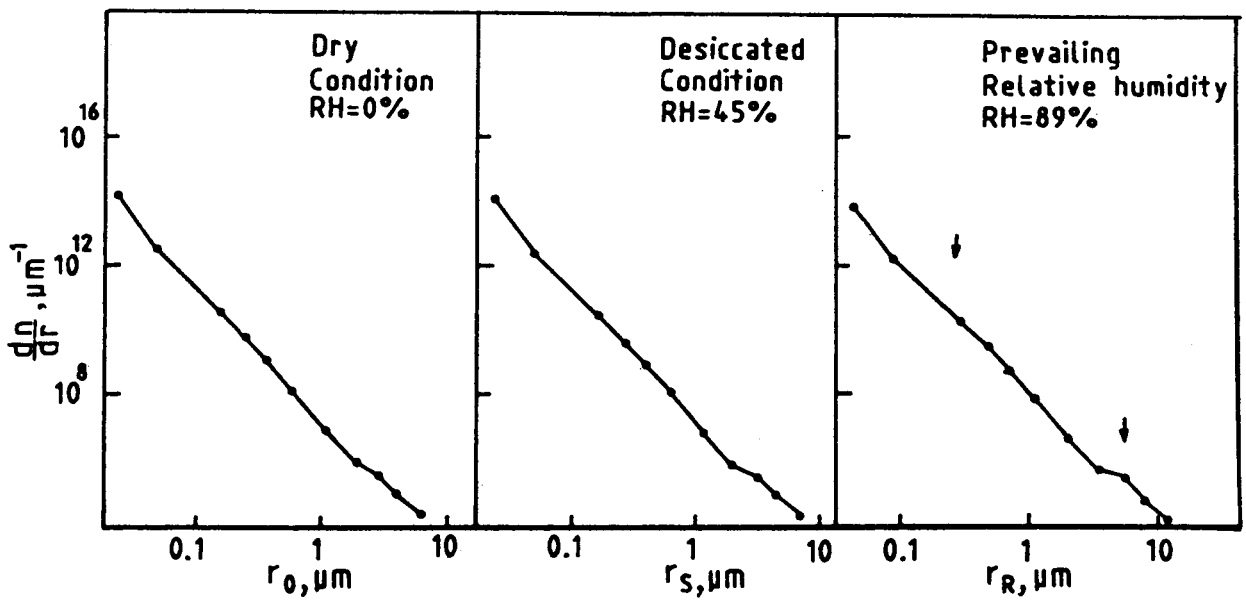

Fig. 5—Aerosol size distributions under dry, desiccated and ambient relative humidity conditions for the samples collected in August 1990.

dition when correction for RH variation is incorporated. Even though the above explained corrections do not change in general the size index significantly, there is a change in the size range of the distribution and the mode radius. When the distribution is not a perfect power law type or the size index varies with change in the particle radius, there will be a noticeable effect in the obtained size index considering a fixed size range of particles. However, the size distribution obtained by incorporating the above said corrections for RH variation is more accurate compared to our earlier reports[16].

Figure 6 shows the number-size distributions of near surface aerosols in different months during the period 1990-93 obtained using the LPI. The nature of the distribution is generally of power law type except for one or two small undulations.

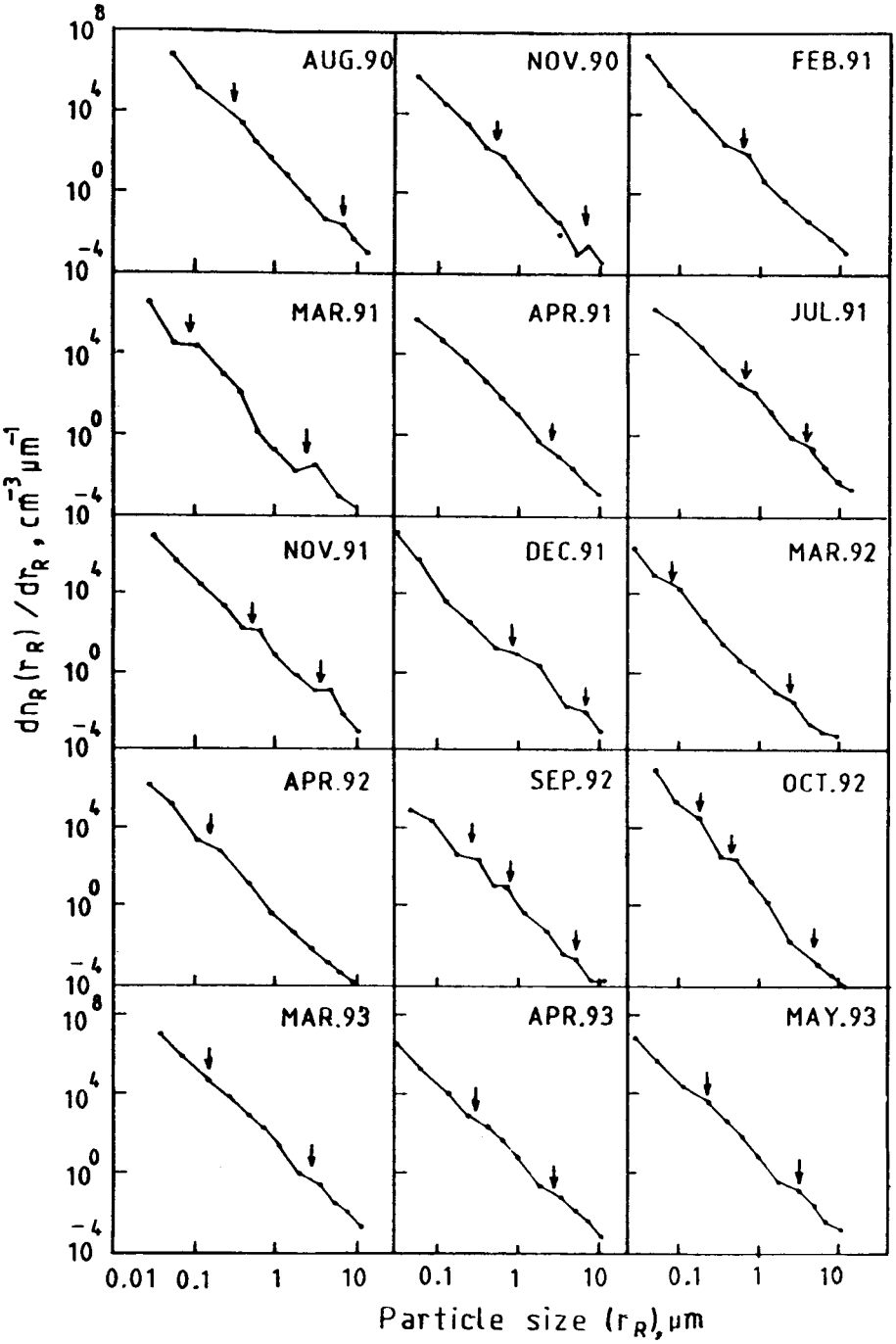

Fig. 6—The number-size distributions of aerosols obtained in different months during the period 1990-93 using the LPI.

These undulations can be attributed to the superposition of a log-normal distribution over the general power law type distribution or a combination of one or more log-normal distributions having different mode radii. All these distributions can be well approximated to a gross power law type for simplicity, and size index of these distributions can be obtained by least square fitting of a power law function to the values of $dn_R(r_R)/dr_R$. The values of size indices for different months obtained by this procedure are depicted in Table 3 along with the values of r_R at which the modes appear in Fig. 6. The near-surface aerosol number density corresponding to each of these sampling is obtained by integrating the corresponding number-size distribution appropriately normalized[16] to unit volume of air. The mean surface relative humidity during each of the above samplings is obtained by averaging the hourly values of the measured surface relative humidity during this period. These values of the mean surface relative humidity and surface aerosol number density corresponding to each month are also presented in Table 3. There is a significant deviation in the estimated surface aerosol number density from our earlier report which can mostly be attributed to the variation in the particle density incorporated in our present analysis. The value of ρ, the particle density, used in our earlier estimates was 2.5 g cm^{-3}, which corresponds to dry conditions, and with the presently added corrections it decreases to 1.24 g cm^{-3} at RH = 90%. The effect of increase in mass (m_s to m_R) is almost neutralized by the corresponding increase in dr, and thus the change in the surface aerosol number density from earlier report is almost inversely proportional to the change in particle density. The seasonal variation of surface aerosol number density shows a distinct minimum during the March-April months and a maximum during the monsoon and winter months. This is in general agreement with the seasonal variation of mixing region aerosol optical depth (0 to 1.1 km) observed at this location employing the CWL experiment[22]. Khemani *et al.*[23] from their impactor measurements at Pune also reported a similar feature on the seasonal variation of aerosol mass loading. The surface aerosol number density was unusually large during March 1993 and low during September 1992.

In most of the months two mode radii appear in the aerosol size distribution. The small particle mode is generally observed around 0.2 μm and the large particle mode around 3-6 μm. In our earlier report this large particle mode was observable only in certain months (March 1991, November 1991, and March 1992), but it became more clear in other months also because of the appropriate corrections for the particle density incorporated in the present analysis. The small particle mode drifts towards the larger size during the winter months. In September 1992 and October 1992 two small particle modes (0.2 μm and 0.7 μm) appeared in the size distribution. The value of this mode radius is minimum ($\sim$0.1 μm) in March for all the three years, whereas in April 1991 this mode is not observed at all. In April 1991 the size

Table 3—Values of mean aerosol size index (ν), mode radius, mean surface relative humidity, and surface aerosol number density obtained from the LPI measurements

Month	Size index (ν)	Mode radius, μm		Surface relative humidity %	Surface aerosol number density $\times 10^5$ cm^{-3}
		1	2		
August 1990	4.00 ± 0.07	0.3	5.9	89 ± 5	1.87
November 1990	4.22 ± 0.20	0.6	6.0	65 ± 4	0.47
February 1991	3.80 ± 0.08	0.6	—	74 ± 7	1.57
March 1991	4.09 ± 0.24	0.1	3.0	67 ± 4	0.67
April 1991	3.95 ± 0.04	—	3.0	66 ± 7	0.59
July 1991	3.79 ± 0.05	0.7	3.9	88 ± 7	1.11
November 1991	3.78 ± 0.10	0.6	4.5	65 ± 4	1.45
December 1991	3.80 ± 0.19	0.8	6.5	67 ± 6	2.67
March 1992	3.89 ± 0.10	0.1	3.0	60 ± 10	0.38
April 1992	4.00 ± 0.08	0.2	—	65 ± 5	0.29
September 1992	3.70 ± 0.12	0.3, 0.7	5.7	83 ± 2	0.10
October 1992	4.43 ± 0.11	0.2, 0.5	5.7	79 ± 7	0.57
March 1993	3.94 ± 0.05	0.1	4.0	76 ± 8	2.83
April 1993	3.96 ± 0.06	0.1	2.5	74 ± 6	0.66
May 1993	3.96 ± 0.06	0.2	2.6	69 ± 4	0.74

distribution was very close to a power law. These results can be compared with the columnar size distribution (CSD) obtained over this station employing a solar radiometer[24]. The CSD indicated the presence of two modes[25], one around 0.1-0.3 μm and the other around 0.9 μm. The first mode (~ 0.2 μm) in CSD matches favourably with the small particle mode observed in the LPI distribution. The mode 2 around 0.9 μm observed in CSD mainly during the winter months matches fairly well with the small particle mode around 0.7 μm observed in the LPI distribution during this period. Thus, in general, the value of the mode radius observed in CSD matches very well with the small particle mode observed in the LPI derived size spectrum. These features also agree fairly well with the observations of Petterson *et al.*[26] in a marine boundary layer employing similar technique. The large particle mode around 3-6 μm observed in the LPI distribution is not seen in CSD which may either be due to the reduced sensitivity of particles above 2 μm radius on the spectral region in which the solar radiometer is operated or due to the fact that the particles contributing to this mode may be confined to a region very close to the earth's surface and thus do not contribute to the observed CSD.

It will be interesting to compare the aerosol size distribution obtained in the present investigation (using LPI) with the 'Navy aerosol model' presented by Gathman[27] using the data from a number of aerosol measurements by different investigators in marine environments. The 'Navy aerosol model' gives the number-size distribution of aerosol particles close to the surface in the radius range 0.01 μm to 10 μm. This size distribution essentially is log-normal type having three modes at 0.03 μm, 0.24 μm and 2 μm respectively (at RH = 80%). The mode around 0.03 μm is attributed to the background aerosol, which is related to the air mass characteristics. Among the other two modes caused by particles of marine origin, the smaller size particles with mode radius ~ 0.24 μm are attributed to those produced by the prevailing high wind conditions. These particles, once introduced into the atmosphere, exhibit a relatively long residence time (related to wind speed history). On the other hand the larger particles with mode radius ~ 2 μm are related to the current wind speeds which are locally generated and seen close to the region where they are produced. Now comparing the size distribution of near surface aerosols obtained using the LPI, in the present investigation, the two mode radii ~ 0.2 μm and 3 μm compare favourably with the two larger size modes of 'Navy aerosol model' caused by particles of marine origin. The small particle mode ~ 0.03 μm (of Navy model) is not observed in the LPI distributions mainly because of the limitation in lower size limit of the measuring system (the lower size limit of the LPI distribution is ~ 0.04 μm). Considering the size range 0.04 μm to 10 μm which is the sensitive range of LPI, the gross form the 'Navy aerosol model' also can be approximated to a power law type. Thus the size distribution of near surface aerosols obtained using the LPI compares favourably with the 'Navy aerosol model' in the overlapping size region and the two mode radii observed in this distribution can be attributed to particles of marine origin.

The values of aerosol size index (ν) obtained from the LPI experiment in the present investigation are nearly the same as those reported earlier[16] (considering the error bars) and generally lie in the range 3.7-4.4. They do not show any systematic variation with season. They also do not show any dependence on surface relative humidity. These values of ν match fairly well with the values reported by different workers[17,28,29] for continental and tropospheric aerosols at lower altitudes by direct sampling technique.

The values of size index ν of the aerosol distribution at an altitude of ~ 190 m above the surface obtained using the CWL experiment on different days during the period 1985 to 1993 are presented in Table 4 along with the surface relative humidity at the time of lidar observation. The

Table 4—Values of size index obtained from CWL experiment along with the respective relative humidities

Date	Size index (ν)	Relative humidity %
21 Mar. 1985	4.5	71
10 Apr. 1985	4.5	74
9 Aug. 1985	5.0	—
2 Sep. 1985	4.5	77
9 Sep. 1985	4.5	77
4 Oct. 1989	3.5	90
9 Nov. 1989	4.5-5.0	71
23 Nov. 1989	4.5-5.0	70
16 Jan. 1990	4.5-5.0	69
14 Feb. 1990	4.5	74
16 Aug. 1990	3.5-4.0	93
11 Oct. 1990	4.0	86
14 Nov. 1990	4.5	69
23 Apr. 1992	4.0	74
21 Oct. 1992	3.5	89
19 Mar. 1993	3.5-4.0	80
21 Apr. 1993	3.5	84
20 May 1993	4.5-5.0	70

size index generally lies in the range 3.5 to 5.0, which is almost the same as that observed for near surface aerosols employing the LPI. These results from the LPI experiment supports the involved assumption of a gross power law type distribution for the mixing region aerosols in estimating the size index from CWL. It also indicates that the size distribution remains almost the same throughout the mixing region which extends over an altitude of ~300 m above the surface at this location. The values of ν shown in Table 3 arrived from the CWL experiment shows a decreasing tendency for large values of RH.

Tables 3 and 4 can be used to compare the results obtained from the two aerosol experiments (LPI and CWL). Though the values of size index obtained from these two experiments are quite comparable and lie almost in the same range considering the error bars, the values in Table 3 do not show any significant dependence on RH whereas those in Table 4 are generally low for higher values of RH. Low value of ν is indicative of the dominance of larger size particles. The difference in the behaviour of the dependence of ν on RH seen from the two experiments is worth examining.

Increase in atmospheric relative humidity makes the aerosol particles to grow in size. As atmospheric aseosols can be considered to be a homogeneous mixture, all the particles will grow with increase in RH in the same fashion. This shifts the particle spectrum as a whole from a given size range to an appropriate larger one. If only this process is active and the size distribution in the entire range follows a simple power law (with same ν throughout), there will not be any change in the size index with changes in RH. Hanel[6] studied the effect of increasing relative humidity on aerosol size distribution and found that the shape of the distribution does not vary significantly until the relative humidity exceeds 95%. At larger relative humidities he observed a broadening of the size distribution which comes from the greater increase (in size) of the larger size particles due to their smaller curvature correction. This causes a small decrease in aerosol size index from 4.1 (at RH = 0 to 75%) to 3.77 (at RH = 95%), which is much smaller than that observed from the CWL experiment. Controlled experiments by Takamura *et al.*[30] also indicated that the volume spectra of aerosols do not change significantly with increase in relative humidity for RH < 85%. For values of RH close to 90% and above they observed an increased growth of larger size particles (> 0.5 μm). In the LPI measurements, the ambient relative humidity varies by $\pm 5\%$ (r.m.s.) during the course of the experiment which will smooth out such small variations in ν with RH. The observed poor dependence of ν on RH in the LPI derived size distributions is in accordance with this. But, if the aerosol size distribution in the entire radius range 0.01-10 μm, instead of following a simple power law with constant ν, follows a distribution having a varying size index (ν being a function of r) and we observe only a portion of this size spectrum covering a fixed size range, as atmospheric relative humidity increases the portion of the size spectrum originally inside the fixed size range will move out and the portion which was lying outside (in the lower size region) will enter into the fixed size range. Conversely, as relative humidity decreases, the portion inside the fixed size range will move out to the lower size region, and the portion of the spectrum which was originally outside (in the larger size region) will move into the fixed size range. In such cases, the size index (ν) derived from the portion of the size spectrum viewed through this fixed range will change with relative humidity. A similar situation is encountered in the case of the CWL experiment. The lidar is operated in the laser wavelength of 514.5 nm. The size range of particles contributing significantly to backscattering in this wavelength is about 0.05 μm to 2 μm (Ref. 31), which will also be true for the angular scattering case used in the present investigation (variation in this range with scattering angle[32] will be rather small for the angles considered in the present study). As the contribution of particles above and below this size range to scattering is small, the size index obtained from CWL will mainly be contributed by the aerosol particles in this region of the size spectrum. When relative humidity increases, particles from the lower size range which were not sensitive earlier will enter into the lidar sensitive range and the particles which were contributing earlier to CWL scattered signals will go out of the lidar sensitivity size range. If the size index is not the same for entire size spectrum of aerosols, thus contributing for scattering at different values of RH, the changes in RH will cause a corresponding change in the lidar derived aerosol size index. To explain the observed variation in Table 4, size index should show a rather smooth increase with increase in particle size near the lidar sensitive size range of 0.05 to 2 μm.

In the above we have discussed different possible reasons for the variation of the aerosol size index with RH. Now, examining the results presented in Tables 3 and 4 in the light of these possible

mechanisms, it can be stated that the size index of the aerosol distribution obtained using the LPI does not show any significant dependence on RH, probably due to the fact that it represents the average distribution for ~6 days during which RH varies by ±5%, causing a smoothening in size index variation with RH. But the size index aloft obtained from the CWL experiment is a spot measurement. The decrease in size index with increase in RH observed in this measurement is more than that expected from the differential growth rate of larger size particles as given by Hanel's theory[10]. Then, the most probable reason which can account for this variation is an increase of the size index with the particle radius in the lidar sensitive size regime.

8 Conclusions

The present study brings out the fact that in obtaining the size distribution and number density using a LPI, the change in relative humidity during the course of the experiment should be accounted appropriately. It also brings out the following features of the aerosol size distribution in the atmospheric mixing region at a tropical coastal station:

(i) The general form of the aerosol size distribution near the surface as well as aloft (~190 m) in the mixing region can be represented by a power law with size index in the range 3.5-5.0.

(ii) Size index of the aerosol distribution near the surface obtained using LPI does not show any dependence on relative humidity, probably due to the fact that it represents an average value for a period of ~6 days. But the size index aloft obtained using CWL showed a decrease with increase in RH, which can mostly be attributed to a change in size index with aerosol size rather than to an increased growth rate of larger size particles.

(iii) In addition to the general power law behaviour, aerosol size distribution near the surface shows the presence of two modes. These modes match fairly well with those in the 'Navy aerosol model' presented by Gathman[27] for a coastal environment. The particles responsible for these modes are mostly of oceanic origin.

(iv) The seasonal variation of number density of aerosols near the surface is similar to that of the mixing region aerosol optical depth.

Acknowledgements

The authors thank Dr B V Krishna Murthy for his valuable suggestions during the preparation of this manuscript. They also acknowledge the valuable support in preconditioning and weighing of the substrates received by them from the Analytical and Spectroscopy Division of VSSC.

References

1 Deepak A & Box G P, cited in *Atmospheric Aerosols: Their Formation, Optical Properties and Effects*, edited by A Deepak (Spectrum, Hampton, Va, USA), 1982.
2 Junge C E, *Air Chemistry and Radioactivity* (Academic Press Inc., New York, USA), 1963.
3 Shettle E P & Fenn R W, *Models of aerosols of the lower atmosphere and the effects of humidity variations on their optical properties*, AFGL-TR-79-0214 (US Air Force Geophysical Laboratory, Hanscom AFB, Massachusetts, USA), 1979.
4 Grassl H, *Tellus (Sweden)*, 25 (1973) 386.
5 Hanel G, *Tellus (Sweden)*, 20 (1968) 371.
6 Hanel G, *J Aerosol Sci (UK)*, 3 (1972) 377.
7 Meszaros A, *Tellus (Sweden)*, 23 (1971) 436.
8 Fitzgerald J W, *J Appl Meteorol (USA)*, 14 (1975) 1044.
9 Kornfeld P, *J Atmos Sci (USA)*, 27 (1970) 256.
10 Hanel G, cited in *Advances in Geophysics*, edited by H E Landsberg and J Van Mieghem (Academic Press Inc, New York, USA), Vol 19, 1976, p 73.
11 Hochrainer D, *J Colloid & Interface Sci (USA)*, 36 (1971) 191.
12 Hanel G & Gravenhorst G, *J Aerosol Sci (UK)*, 4 (1974) 47.
13 Anderson A A, *Am Ind Hyg Ass J (USA)*, 27 (1966) 160.
14 Ward G, Cushing K M, McPeters R D & Green A E S, *Appl Opt (USA)*, 21 (1973) 2585.
15 King M D, Byrne D M, Herman B M & Regan J A, *J Atmos Sci (USA)*, 35 (1978) 2153.
16 Parameswaran K & Vijayakumar G, *Indian J Radio & Space Phys*, 22 (1993) 42.
17 Goel R K, Varshneya N C & Verma T S, *Ann Geophys (France)*, 3 (1985) 339.
18 Pruppacher H R & Klett J D, *Microphysics of clouds and precipitation* (D Reidal Publishing Co, Hingham, Massachusetts, USA), 1978.
19 McClatchy R A, Fenn R W, Selby J E A, Volz F E & Garing J S, *Optical properties of the atomsphere*, AFCRL-72-0497 (US Air Force Geophysical Laboratory, Hanscom AFB, Massachusetts, USA), 1972.
20 Parameswaran K, Rose K O & Kirshna Murthy B V, *J Geophys Res (USA)*, 89 (1984) 2541.
21 Reist P C, *Introduction to aerosol science* (Macmillan Publishing Co, New York, USA), 1984.
22 Parameswaran K, Vijayakumar G, Krishna Murthy B V & Krishna Moorthy K, *Ann Geophys (France)*, 12 (1994), in press.
23 Khemani L T, Momin G A, Naik M S, Vijayakumar R & Ramana Murthy Bh V, *Tellus (Sweden)*, 34 (1982) 151.
24 Krishna Moorthy K, Prabha B Nair & Kirshna Murthy B V, *J Appl Meteorol (USA)*, 30 (1991) 844.
25 Prabha B Nair, *Studies on atmospheric aerosols*, Ph D thesis, University of Kerala, Thiruvananthapuram, India, 1993.
26 Patterson E M, Kaing C S, Delany A C, Wartburg A F, Lesli A C & Huebert B J, *J Geophys Res (USA)*, 85 (1980) 7361.
27 Gathman S G, *Opt Eng Bellingham (USA)*, 22 (1983) 57.
28 Pasceri R E & Friedlander S K, *J Atmos Sci (USA)*, 22 (1965) 579.
29 Blifford I H & Ringer L D, *J Atmos Sci (USA)*, 26 (1969) 716.
30 Takamura T, Tanaka M & Nakajima T, *J Meteorol Soc Jpn (Japan)*, 62 (1984) 573.
31 Muller H & Quenzel H, *Appl Opt (USA)*, 24 (1985) 648.
32 Thomalla E & Quenzel H, *Appl Opt (USA)*, 21 (1982) 3170.